
Dynamic Spatio-Temporal Graph Neural Network for Early Detection of Pornography Addiction in Adolescents Based on Electroencephalogram Signals

Achmad Ardani Prasha^{1*} Clavino Ourizqi Rachmadi¹ Sabrina Laila Mutiara¹
Hilman Syachr Ramadhan¹ Chareyl Reinalyta Borneo² Saruni Dwiasnati¹

¹Faculty of Computer Science, Universitas Mercu Buana, West Jakarta, Indonesia

²Faculty of Psychology, Universitas Mercu Buana, West Jakarta, Indonesia

Abstract

Adolescent pornography addiction requires early detection based on objective neurobiological biomarkers because self-report is prone to subjective bias due to social stigma. Conventional machine learning has not been able to model dynamic functional connectivity of the brain that fluctuates temporally during addictive stimulus exposure. This study proposes a state-of-the-art Dynamic Spatio-Temporal Graph Neural Network (DST-GNN) that integrates Phase Lag Index (PLI)-based Graph Attention Network (GAT) for spatial modeling and Bidirectional Gated Recurrent Unit (BiGRU) for temporal dynamics. The dataset consists of 14 adolescents (7 addicted, 7 healthy) with 19-channel EEG across 9 experimental conditions. Leave-One-Subject-Out Cross Validation (LOSO-CV) evaluation shows F1-Score of $71.00\% \pm 12.10\%$ and recall of 85.71% , a 104% improvement compared to baseline. Ablation study confirms temporal contribution of 21% and PLI graph construction of 57%. Frontal-central regions (Fz, Cz, C3, C4) are identified as dominant biomarkers with Beta contribution of 58.9% and Hjorth of 31.2%, while Cz-T7 connectivity is consistent as a trait-level biomarker for objective screening.

Keywords: pornography addiction, graph neural network, electroencephalogram, biomarker, child protection

1 Introduction

Pornography addiction in adolescents is a public health problem that is increasingly concerning in the digital era. Data from the National Survey on Children and Adolescent Life Experiences (SNPHAR) from the Ministry of Women Empowerment and Child Protection (Kementerian PPPA, 2021) shows that 66.6% of boys and 62.3% of girls aged 13–17 years in Indonesia are exposed to online pornographic content. According to Faisal et al. (2022) and Adarsh and Sahoo (2023), this condition risks disrupting prefrontal cortex development which plays a role in executive functions, decision-making, and impulse control. Therefore, implementation of protection through objective and accurate early detection methods is needed to identify adolescents who are at risk or have experienced pornography addiction so that intervention can be done as early as possible.

Conventional screening methods such as Young’s Pornography Addiction Screening Test (YPAST) have significant limitations in the form of self-report bias and social desirability. Based on Privara and Bob (2023), pornography consumption can induce cognitive-affective distress, guilt, and moral conflict. Therefore, objective biomarkers that can measure neurobiological changes due to pornography addiction without relying on subjective reports are needed.

*Corresponding author: 41523010005@student.mercubuana.ac.id

Huang et al. (2025) and Bouhadja and Bouramoul (2022) proved that Electroencephalogram (EEG) is effective in detecting brain activity changes related to various types of addiction. This can include utilizing public Electroencephalogram datasets from adolescents with and without pornography addiction provided by Kang et al. (2021). Sun et al. (2022) have shown significant advances in applying deep learning based on Convolutional Neural Network (CNN) for EEG data analysis on addiction problems. However, Huang et al. (2025) noted that most other research is still dominated by traditional machine learning such as Support Vector Machine (SVM), Random Forest (RF), and Multi-Layer Perceptron (MLP) using static features, so they have not been able to capture temporal dynamics and functional connectivity between brain regions. In fact, Brand et al. (2016) emphasized that the brain is a complex dynamic system with fluctuating connectivity, especially when exposed to addictive stimuli. This is reinforced by the Interaction of Person-Affect-Cognition-Execution (I-PACE) model from Brand et al. (2019) which highlights the importance of understanding temporal dynamics in addictive behavior.

Graph Neural Network (GNN) has proven superior in modeling relationally structured data such as EEG signals representing brain connectivity networks (Abadal et al., 2025; Graña and Morais-Quilez, 2023; Xue et al., 2024). Recent reviews show GNN potential in EEG analysis for various applications, especially emotion detection (Almohammadi and Wang, 2024; Klepl et al., 2024) and psychiatric disorders (Liu and Zhao, 2025), although its application for pornography addiction detection has never been explored. Therefore, this study proposes a Dynamic Spatio-Temporal Graph Neural Network (DST-GNN) architecture that integrates Graph Attention Network (GAT) for modeling spatial brain connectivity based on Phase Lag Index (PLI). According to Stam et al. (2007), this metric is chosen because it is robust against volume conduction artifacts. In addition, Bidirectional Gated Recurrent Unit (BiGRU) is also used to capture temporal dynamics of neural activity. Bidirectional RNN architecture has proven effective for EEG sequence analysis, both using Bi-LSTM (Algarni et al., 2022; Jusseaume and Valova, 2022) and GRU (Cho et al., 2014). Walther et al. (2023) comprehensively compared various deep learning architectures for EEG time series analysis. The main novelty of this research is the first application of GNN on pornography addiction detection, integration of PLI metrics in graph construction, and dynamic modeling of brain connectivity across time.

The objectives of this study are: (1) to develop a DST-GNN model for EEG-based pornography addiction classification, (2) to identify neurobiological biomarkers in the form of brain regions and connectivity patterns that are most discriminative through explainability analysis, and (3) to analyze brain connectivity differences across various cognitive and emotional conditions.

2 Methods

This study uses a quantitative experimental approach with a cross-sectional design to develop and evaluate the DST-GNN model in detecting pornography addiction based on EEG signals. The research methodology is systematically arranged through several integrated stages, including: data acquisition, preprocessing, feature extraction, graph construction, model development, hyperparameter optimization, evaluation, and explainability analysis.

Figure 1 presents the research design flowchart comprehensively. The research pipeline consists of six main phases: (1) Data phase includes EEG dataset acquisition from Mendeley Data; (2) Preprocessing phase includes bandpass filter, notch, normalization, and windowing; (3) Features phase includes Power Spectral Density (PSD) extraction and Hjorth parameters as well as PLI graph construction; (4) Modeling phase includes DST-GNN and baseline model training; (5) Evaluation phase uses LOSO-CV and ablation study; (6) Analysis phase includes explainability and biomarker identification. The data flow follows transformation from 14 subjects with 19 EEG channels to produce binary classification with F1-Score 71% and recall 86%.

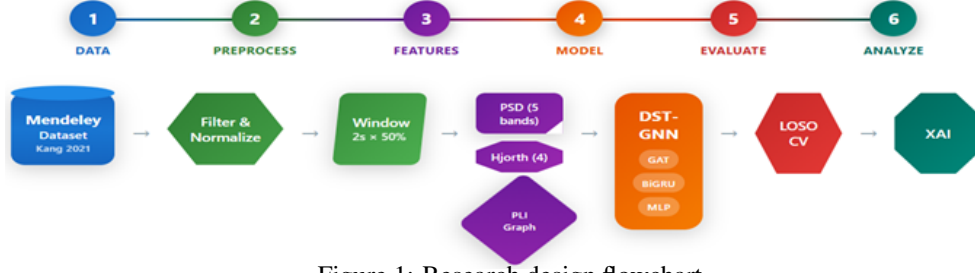


Figure 1: Research design flowchart

Figure 2 displays the DST-GNN architecture in detail. The model consists of three main integrated components: (1) Spatial Encoder using two Graph Attention Network (GAT) layers with 2 attention heads and hidden dimension 64 for modeling spatial connectivity between EEG channels (Veličković et al., 2018; Venu and Natesan, 2024); (2) Temporal Encoder using Bidirectional GRU (BiGRU) 2 layers with hidden dimension 128 for capturing temporal dynamics of graph sequences; and (3) Classifier in the form of Multi-Layer Perceptron (MLP) with dropout 0.5 for binary classification. Input is 19-channel EEG signals transformed into 30 temporal windows with 9 features per node (consisting of 5 PSD bands + 4 Hjorth parameters).

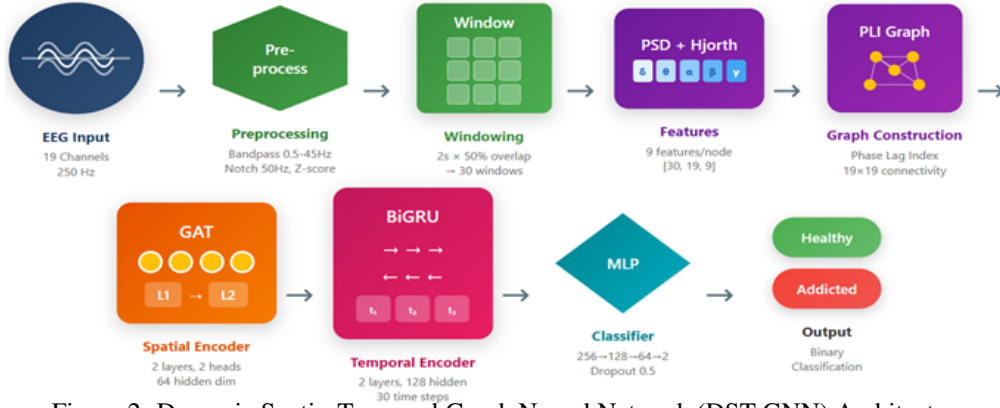


Figure 2: Dynamic Spatio-Temporal Graph Neural Network (DST-GNN) Architecture

Spatial Encoder uses Graph Attention Network (GAT) 2-layer with multi-head attention mechanism to compute node representations based on neighbor features with adaptive attention weights according to Equations (1) and (2):

$$\alpha_{ij} = \text{softmax}(\text{LeakyReLU}(\mathbf{a}^T [\mathbf{W}\mathbf{h}_i \parallel \mathbf{W}\mathbf{h}_j])) \quad (1)$$

$$\mathbf{h}'_i = \sigma \left(\sum_{j \in \mathcal{N}_i} \alpha_{ij} \mathbf{W}\mathbf{h}_j \right) \quad (2)$$

where α_{ij} is the attention coefficient, \mathbf{W} is the learnable weight matrix, \mathbf{h}_i and \mathbf{h}_j are node features of node i and j , and \mathcal{N}_i is the neighborhood of node i in the PLI graph.

Temporal Encoder uses Bidirectional Gated Recurrent Unit (BiGRU) 2-layer to model graph sequence dynamics according to Equations (3)–(6):

$$\mathbf{z}_t = \sigma(\mathbf{W}_z \cdot [\mathbf{h}_{t-1}, \mathbf{x}_t]) \quad (3)$$

$$\mathbf{r}_t = \sigma(\mathbf{W}_r \cdot [\mathbf{h}_{t-1}, \mathbf{x}_t]) \quad (4)$$

$$\tilde{\mathbf{h}}_t = \tanh(\mathbf{W} \cdot [\mathbf{r}_t \odot \mathbf{h}_{t-1}, \mathbf{x}_t]) \quad (5)$$

$$\mathbf{h}_t = (1 - \mathbf{z}_t) \odot \mathbf{h}_{t-1} + \mathbf{z}_t \odot \tilde{\mathbf{h}}_t \quad (6)$$

where \mathbf{z}_t is the update gate, \mathbf{r}_t is the reset gate, \mathbf{h}_{t-1} is the previous hidden state, \mathbf{x}_t is input at time t , $\tilde{\mathbf{h}}_t$ is the candidate hidden state, and \mathbf{h}_t is the output hidden state.

Model training was performed using NVIDIA A100-SXM4-40GB GPU with 42.4 GB memory. Hyperparameter optimization uses the Optuna framework with 30 trials and automatic pruning. The

best parameters were found at trial 12 with composite score $(0.6 \times \text{accuracy} + 0.4 \times F1) = 0.6524$: learning rate: 0.000668, hidden dimension: 64, GAT heads: 2, GRU layers: 2, GRU hidden: 128, dropout: 0.182, weight decay: 3.53×10^{-5} . AdamW optimizer with Cosine Annealing learning rate scheduler was applied for more stable convergence. Early stopping with patience 15 epochs was applied to prevent overfitting. Evaluation uses Leave-One-Subject-Out Cross-Validation (LOSO-CV) (Allgaier and Pryss, 2024) with 3 random seeds (42, 123, 456) to ensure result reliability.

In addition to the DST-GNN model, five baseline models were also evaluated for comparison: Logistic Regression with L2 regularization, Support Vector Machine (SVM) with RBF (Radial Basis Function) kernel, Random Forest (RF) with 100 estimators, XGBoost with default parameters, and Multi-Layer Perceptron (MLP) with 256-128-64 neuron architecture. All baselines use the same features (PSD + Hjorth + correlation) with LOSO-CV evaluation.

The research dataset was obtained from Mendeley Data collected by Kang et al. (2021). The dataset consists of EEG recordings from 14 adolescent participants aged 13-15 years, divided into 7 participants with pornography addiction (YPAST score ≥ 36) and 7 healthy participants as controls. Recording was performed using a 19-channel EEG system with electrode placement following the International 10-20 System standard at 250 Hz sampling frequency. Electrode placement follows the International 10-20 System standard which is an international standard system for EEG electrode placement. This system divides the head into areas based on percentage of distance between anatomical reference points. Figure 3 shows the positions of 19 electrodes (Fp1, Fp2, F7, F3, Fz, F4, F8, T7, C3, Cz, C4, T8, P7, P3, Pz, P4, P8, O1, O2) used in EEG data acquisition.

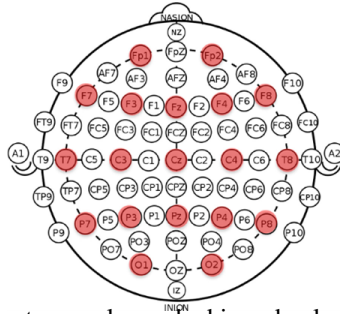


Figure 3: Electrode placement on scalp marked in red color (Source: Kang et al. (2021))

Table 1 shows details of EEG signals recorded for each subject, including task name, file name, recording duration, and data dimensions in the form of samples \times channels. Each participant underwent 9 experimental conditions designed to evaluate brain responses to various stimuli: Eyes Closed (EC), Eyes Open (EO), Happy (H), Calm (C), Sad (S), Fear (F), Memorize (M), Executive Task (ET) with pornographic stimulus exposure, and Recall (R). Total recording duration per subject is 10 minutes with 250 Hz sampling frequency.

Table 1: EEG signal recording details per experimental condition (Source: Kang et al. (2021))

No.	Task Name	File Name	Duration (s)	Samples \times Channels
1	Eyes Closed	EC.csv	60	15,000 \times 19
2	Eyes Open	EO.csv	60	15,000 \times 19
3	Happy	H.csv	60	15,000 \times 19
4	Calm	C.csv	60	15,000 \times 19
5	Sad	S.csv	60	15,000 \times 19
6	Fear	F.csv	60	15,000 \times 19
7	Memorise 15 words	M.csv	60	15,000 \times 19
8	Executive Tasks	ET.csv	120	30,000 \times 19
9	Recall 15 words	R.csv	60	15,000 \times 19

The dataset is stored in an organized folder structure with the main folder data_porn_addiction containing 14 subfolders (S1-S14) for each subject as shown in Figure 4. Each subject folder contains .csv files for each experimental task (EC.csv, EO.csv, H.csv, C.csv, S.csv, F.csv, M.csv, ET.csv, R.csv). Additional information such as channel representation, acquisition device, participant labels, and experimental protocol details are also available.

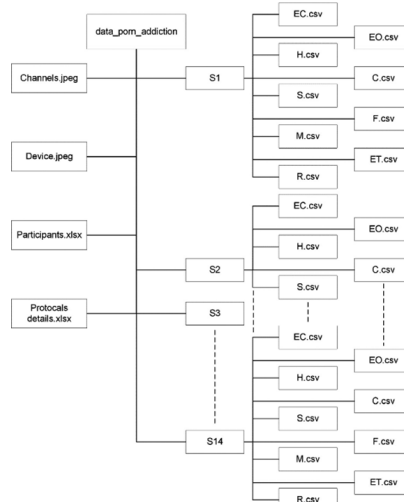


Figure 4: Dataset folder structure (Source: Kang et al. (2021))

Table 2 shows participant details involved in data collection, including subject ID, gender, and classification label (Addicted or Not Addicted) based on YPAST screening results verified by clinical psychologists.

Table 2: Participant details (Source: Kang et al. (2021))

No.	Subject ID	Gender	Label
1	S1	Male	Addicted
2	S2	Female	Not Addicted
3	S3	Female	Not Addicted
4	S4	Male	Not Addicted
5	S5	Male	Addicted
6	S6	Male	Addicted
7	S7	Male	Not Addicted
8	S8	Male	Not Addicted
9	S9	Female	Addicted
10	S10	Female	Addicted
11	S11	Female	Addicted
12	S12	Male	Not Addicted
13	S13	Male	Not Addicted
14	S14	Male	Addicted

The ET condition is the main focus of analysis because it involves direct exposure to pornographic stimuli, but multi-condition analysis was also performed to identify consistent biomarkers. Figure 5 shows balanced data distribution at the subject level (7:7) with a total of 420 temporal windows after preprocessing.

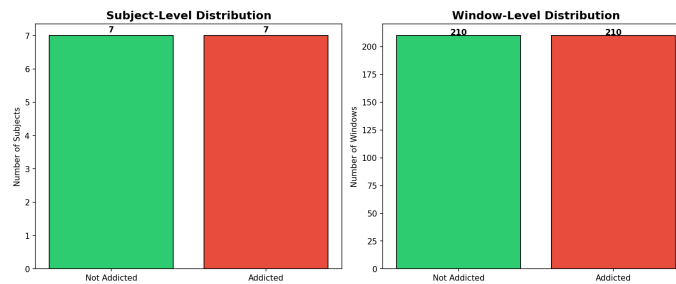


Figure 5: Data distribution at subject level (left) and window level (right)

EEG signal preprocessing was performed through several stages. First, a 4th order Butterworth bandpass filter was applied with cutoff frequency 0.5-45 Hz to remove low frequency noise (drift) and high frequency noise (muscle artifact, powerline). A notch filter at 50 Hz was applied to remove electrical interference. Furthermore, signals were normalized using z-score normalization per channel

calculated according to Equation (7):

$$z = \frac{x - \mu}{\sigma} \quad (7)$$

where x is the amplitude value, μ is the mean, and σ is the channel standard deviation. Figure 6 shows comparison of filtered EEG signals (first window, 2 seconds) between healthy and addicted subjects on five representative channels (Fp1, Fz, Cz, Pz, O1), with the left panel showing non-addicted subject (S2) in green and the right panel addicted subject (S1) in orange-red, y-axis showing amplitude (μV) and x-axis time (seconds), which generally shows that the addicted group has higher and more irregular amplitude fluctuations—especially on Fp1 channel—while the healthy group displays more stable drift patterns on Fz and more consistent Cz oscillations compared to high variability in the addicted group.

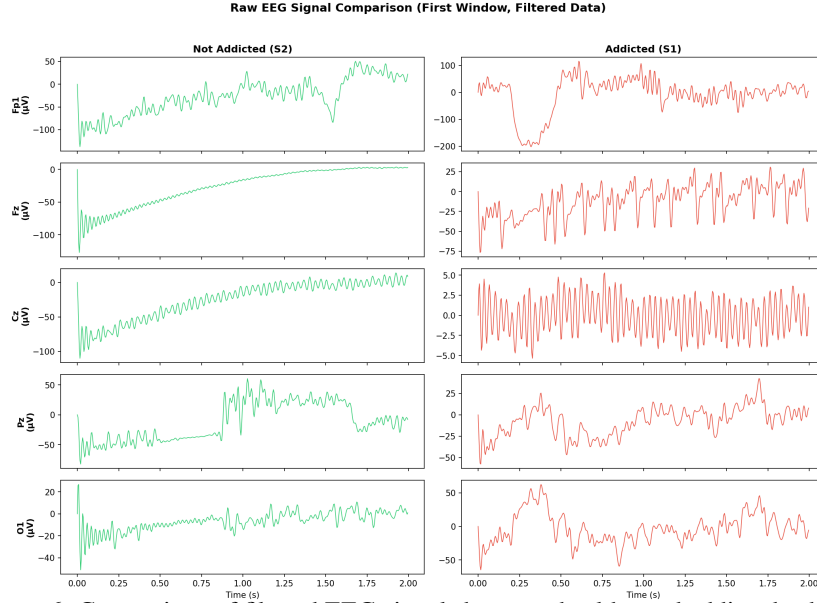


Figure 6: Comparison of filtered EEG signals between healthy and addicted subjects

Two categories of features were extracted from each EEG window. First, PSD was calculated using Welch’s method (Chaddad et al., 2023; Welch, 1967) on 5 standard frequency bands: Delta (0.5–4 Hz), Theta (4–8 Hz), Alpha (8–13 Hz), Beta (13–30 Hz), and Gamma (30–45 Hz). Second, Hjorth parameters (Hjorth, 1970) were extracted including activity (signal variance), mobility (ratio of first derivative standard deviation to original signal), complexity (ratio of first derivative mobility to signal mobility), and mean amplitude. A total of 9 features were extracted per channel, yielding 171 node features.

Figures 7 and 8 present comprehensive spectral analysis revealing important differences between the two groups. Figure 7 consists of two panels: the left panel shows global PSD comparison in logarithmic scale with green line (not addicted) and red (addicted) above colored background showing frequency bands (Light Blue: Delta (0 - 4 Hz), Light Purple: Theta (4 - 8 Hz), Light Orange: Alpha (8 - 13 Hz), Light Green: Beta (13 - 30 Hz), Pink: Gamma (> 30 Hz)); the right panel shows PSD difference with red shading (higher in addicted) and green (higher in not addicted). It can be seen that the addicted group shows increased power in the Beta band (13-30 Hz) associated with arousal and cognitive processes, consistent with prefrontal cortex hyperactivation theory in addiction. Figure 8 displays a 3×5 matrix of scalp topomaps showing spatial distribution of band power, with the most significant differences concentrated in frontal and central regions.

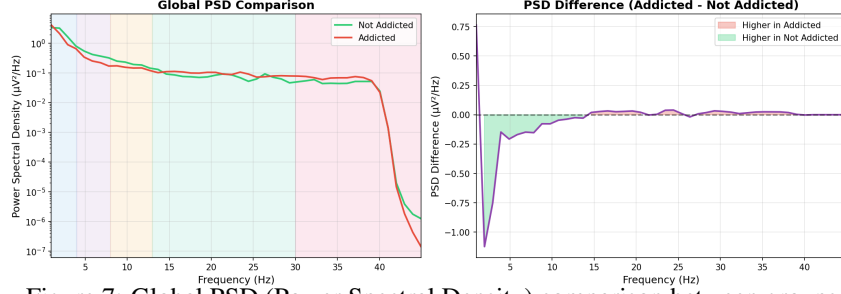


Figure 7: Global PSD (Power Spectral Density) comparison between groups

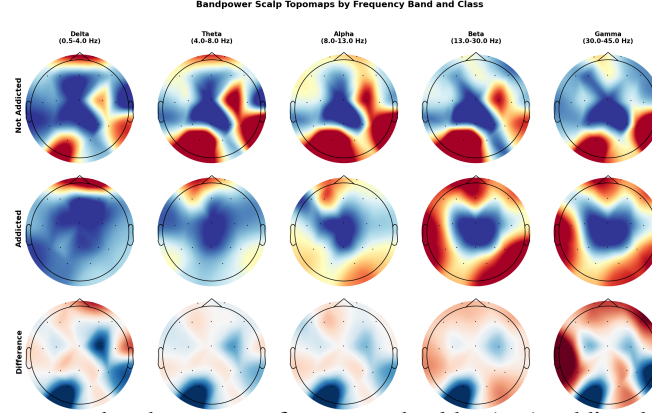


Figure 8: Scalp topomaps band power per frequency: healthy (top), addicted (middle), difference (bottom)

Brain connectivity graphs were constructed using Phase Lag Index (PLI) which measures the asymmetry of phase difference distribution between two signals (Stam et al., 2007). PLI is defined according to Equation (8):

$$\text{PLI} = |\langle \text{sign}(\Delta\phi(t)) \rangle| \quad (8)$$

where $\Delta\phi(t)$ is the instantaneous phase difference between two signals at time t , and $\langle \cdot \rangle$ indicates temporal average. PLI ranges from 0-1, with high values indicating strong functional connectivity (Stam et al., 2007). The advantage of PLI over conventional coherence metrics is its robustness against volume conduction artifacts (Krukow et al., 2024; Polat, 2023). The application of PLI in adolescent neuroimaging contexts has also been validated by recent research (Raveendran et al., 2025). Additionally, weighted PLI (wPLI) was also calculated according to Equation (9) for more robust multi-condition analysis (Yan et al., 2021):

$$\text{wPLI} = \frac{|\langle |\Delta\phi(t)| \cdot \text{sign}(\Delta\phi(t)) \rangle|}{\langle |\Delta\phi(t)| \rangle} \quad (9)$$

Graph $G = (V, E)$ was constructed with V as the set of 19 nodes (EEG channels) and E as PLI-weighted edges. Thresholding at the 50th percentile was applied to retain the most significant connections. Figure 9 illustrates the EEG graph construction of subject 1 (addicted) through visualization of 19-channel graph topology based on Phase Lag Index (PLI) values showing 56 of 107 strongest edges (Top 50%), 19×19 PLI matrix representing functional connectivity strength, and node feature heatmap consisting of 9 features (5 PSD bands and 4 Hjorth parameters) on each channel, while Figure 10 shows temporal evolution of brain connectivity of the same subject on several time windows, confirming the dynamic character of functional connectivity successfully captured by the model.

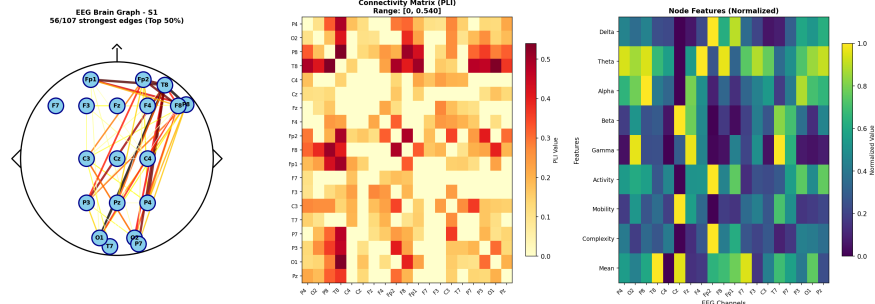


Figure 9: EEG graph structure: connection topology (left), PLI matrix (center), node features (right)

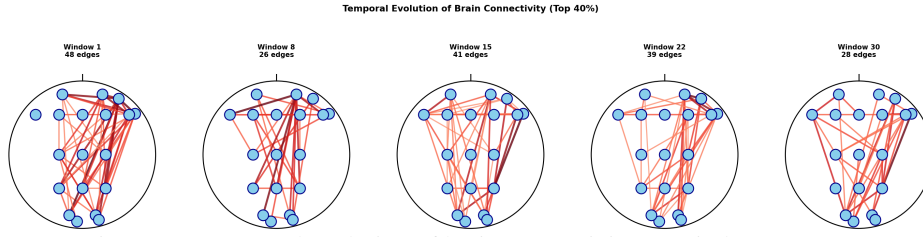


Figure 10: Temporal evolution of brain connectivity on window sequence

Figure 11 presents direct comparison of brain connectivity patterns between two subjects using top 50% strongest connection graph visualization with different color schemes to distinguish groups. Analysis shows substantial differences: healthy subject (S2) has 66 strong edges with more evenly distributed connectivity patterns across brain regions, while addicted subject (S1) only has 48 strong edges with higher concentration in the right frontal-temporal region (F4, F8, T8). This pattern indicates brain network reorganization in addicted individuals, where there is decreased global connectivity but increased local clustering in regions involved in reward processing and impulse control. These findings are consistent with allostatic theory of addiction showing a shift from homeostatic regulation to pathological conditions.

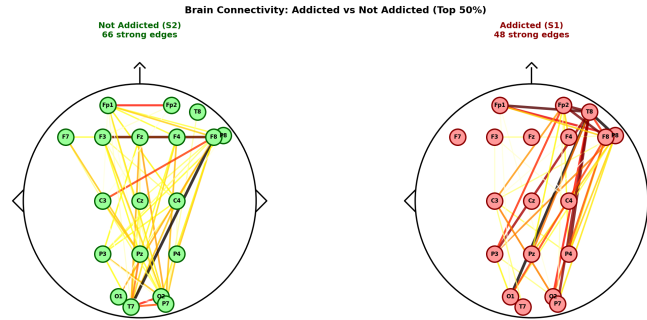


Figure 11: Brain connectivity pattern comparison: healthy (left, 66 edges) vs addicted (right, 48 edges)

3 Results and Discussion

This section presents comprehensive evaluation results of the DST-GNN model compared to baselines, ablation analysis to validate component contributions, and explainability analysis for model decision interpretation. Results are discussed in the context of neuroimaging findings related to addiction and implications for child protection. The complete implementation is available at the GitHub repository: <https://github.com/achmadardanip/eeg-research/tree/master>.

Table 3 shows baseline model evaluation results using LOSO-CV. Logistic Regression achieves the best performance with 62.14% accuracy and 34.73% F1-Score. All baseline models show low recall (<30%), indicating difficulty in detecting positive cases (addiction). This is due to limitations of static features that cannot capture temporal dynamics of brain connectivity.

Table 3: Baseline model evaluation results (LOSO-CV)

Model	Accuracy	Precision	Recall	F1-Score	ROC-AUC
Logistic Regression	62.14%	50.00%	29.29%	34.73%	50.00%
SVM (RBF)	58.33%	50.00%	28.57%	34.37%	50.00%
Random Forest	44.52%	42.86%	16.43%	20.63%	50.00%
XGBoost	49.29%	50.00%	20.71%	26.04%	50.00%
MLP	51.90%	50.00%	26.19%	32.46%	50.00%

Figure 12 visualizes baseline performance comparison with error bars. It can be seen that all models show high variability and suboptimal performance, especially on the recall metric which is critical for medical screening contexts where minimizing false negatives is very important.

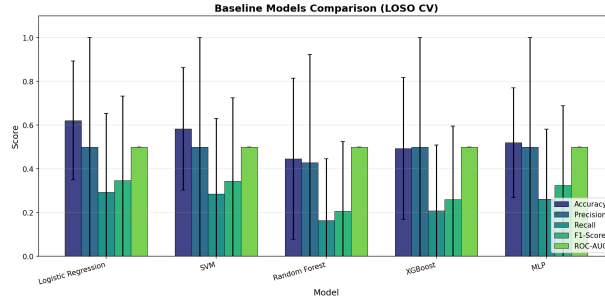


Figure 12: Baseline model performance comparison with error bars

Table 4 shows DST-GNN evaluation results with multi-seed LOSO-CV. DST-GNN achieves an average F1-Score of $71.00\% \pm 12.10\%$, a 104% improvement compared to the best baseline. High recall (85.71%) is very important for screening contexts where minimizing false negatives is prioritized. Inter-seed variability reflects sensitivity to initialization, but performance is consistently better than baselines.

Table 4: DST-GNN multi-seed LOSO-CV evaluation results

Seed	Accuracy	Precision	Recall	F1-Score	ROC-AUC
42	57.14%	54.55%	85.71%	66.67%	59.18%
123	78.57%	77.78%	100.00%	87.50%	89.80%
456	57.14%	50.00%	71.43%	58.82%	44.90%
Mean \pm SD	64.29 \pm 15.43%	60.77 \pm 12.17%	85.71 \pm 11.66%	71.00 \pm 12.10%	64.63 \pm 18.73%

Figure 13 displays the confusion matrix and DST-GNN performance metrics. Prediction distribution shows that the model tends to classify to the positive class (addiction), yielding high recall but with a trade-off on precision. Figure 14 displays ROC curves for each seed, with seed 123 achieving the highest Area Under the Curve (AUC) of 0.898.

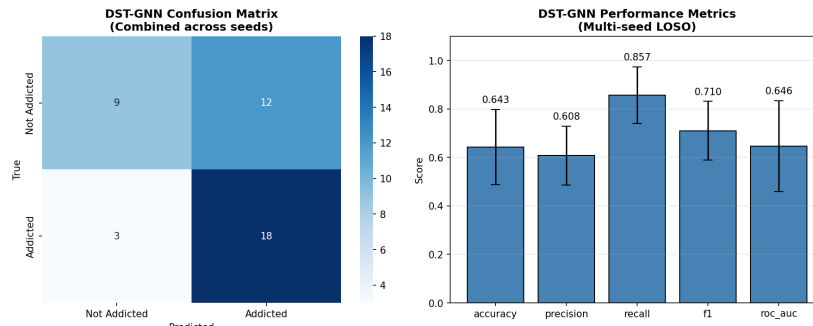


Figure 13: Confusion matrix (left) and DST-GNN performance metrics (right)

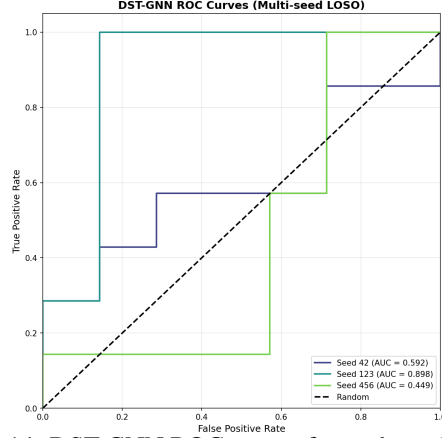


Figure 14: DST-GNN ROC curves for each random seed

Ablation study was conducted to validate the contribution of each DST-GNN component. Table 5 shows that removal of temporal component (BiGRU) decreases F1-Score by 21%, confirming the importance of modeling temporal dynamics of brain activity. Replacing PLI graph with fully-connected graph causes drastic F1-Score decrease (57%), showing that functional connectivity-based graph construction is very critical for model performance.

Table 5: DST-GNN ablation study results

Configuration	Accuracy	F1-Score	F1 Change
Full DST-GNN	64.29%	71.00%	Baseline
Spatial-Only (without BiGRU)	42.86%	50.00%	-21.00%
Fully-Connected (without PLI)	14.29%	14.29%	-56.71%

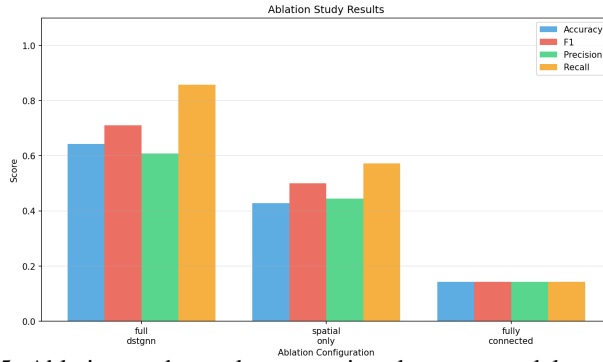


Figure 15: Ablation study results comparison between model configurations

Explainability analysis was conducted to identify brain regions and features that contribute most to model predictions. Figure 16 shows channel importance topomap where frontal (Fz, Fp2) and central (Cz, C3, C4) regions have the highest importance. These findings are consistent with neuroimaging literature showing prefrontal cortex involvement in impulse regulation and reward processing in addiction.

Figure 17 displays feature importance revealing the largest contribution from the Beta frequency band (58.9%) associated with cognitive processes and arousal, followed by Hjorth parameters (31.2%) measuring temporal signal characteristics. Beta dominance is consistent with findings that addiction causes changes in high-frequency activity related to cognitive control.

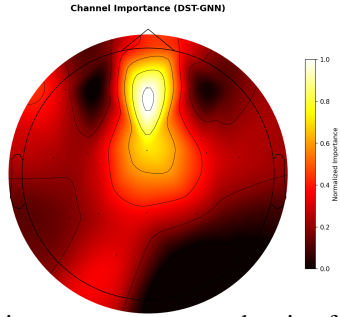


Figure 16: DST-GNN channel importance topomap showing frontal-central region dominance

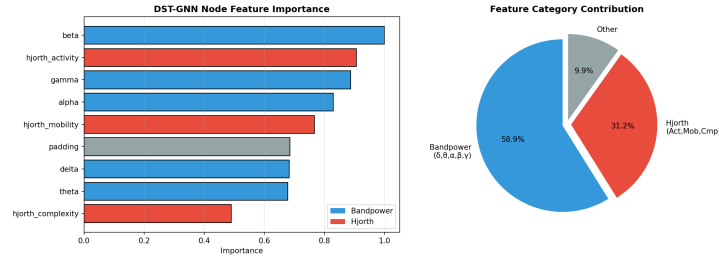


Figure 17: DST-GNN feature importance: Beta and Hjorth Activity as main features

Functional connectivity analysis was performed on all 9 experimental conditions using wPLI to identify consistent and condition-specific patterns. Figure 18 shows wPLI connectivity differences between addicted and healthy groups on 9 experimental conditions. Red color indicates increased connectivity in the addicted group, while blue indicates decrease. In baseline conditions (EC, EO), increased global connectivity is seen in the addicted group. Emotional conditions (H, C, S, F) show heterogeneous patterns with increase in central-temporal connections. Cognitive conditions (M, R) and Executive Task (ET) show the most significant increase in C4-T7, Cz-C3, and C4-C3 connections, indicating hyperconnectivity in regions involved in reward processing and cognitive control.

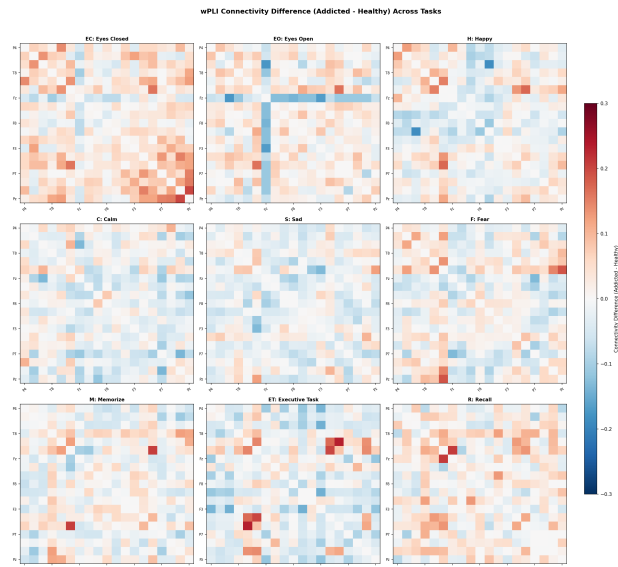


Figure 18: wPLI connectivity differences (Addicted - Healthy) on 9 experimental conditions

An important finding of this research is the Cz-T7 connection which shows consistent differences across various conditions (EC, EO, H, M), indicating a trait-level biomarker that does not depend on specific experimental conditions. Several studies report functional brain activity changes related to pornography consumption and addiction, particularly involving temporal and frontal regions (Prantner et al., 2024; Privara and Bob, 2023; Shu et al., 2025). These findings open opportunities for developing objective detection approaches that do not depend on pornographic stimulus exposure during examination.

Figure 19 presents band power analysis per condition category. The addicted group shows lower power in Alpha and Theta bands across various conditions. Significant differences ($p < 0.05$) were found in memorize condition (Alpha $p = 0.0002$; Theta $p = 0.0014$), fear (Alpha $p = 0.0029$; Gamma $p = 0.0192$ higher in addicted), and calm (Alpha $p = 0.0044$). Decreased Alpha is related to reduced emotional regulation ability, consistent with the I-PACE model.

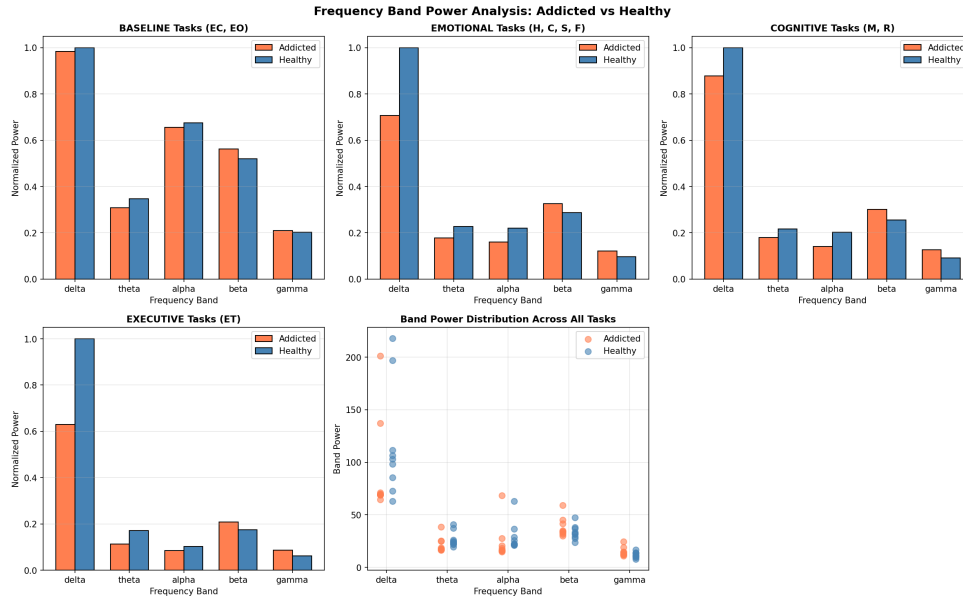


Figure 19: Band power analysis per condition category: baseline, emotional, cognitive, executive

Figure 20 displays brain region discriminability between tasks, confirming that central regions (C3, Cz, C4) are most consistently discriminative across various conditions. Figure 21 shows global connectivity metrics revealing interesting patterns: the addicted group has higher connectivity in baseline conditions but lower in emotional conditions, indicating context-dependent network dysregulation.

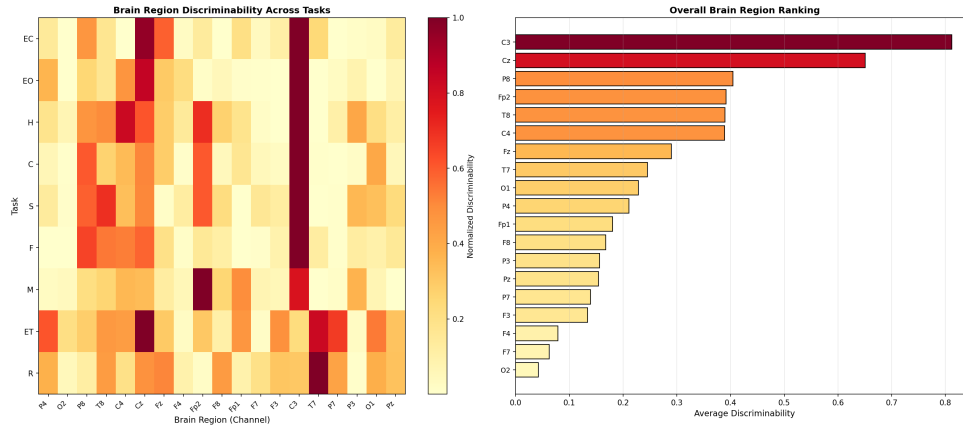


Figure 20: Brain region discriminability between tasks (left) and overall ranking (right)

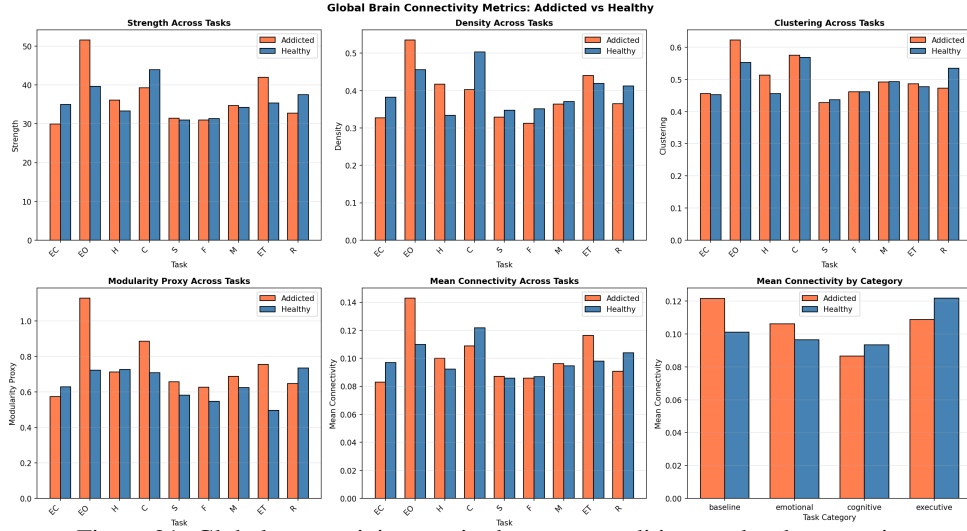


Figure 21: Global connectivity metrics between conditions and task categories

Advanced explainability analysis using Integrated Gradients (IG) (Cui et al., 2023; Farahani et al., 2022) and gradient-based edge importance provides more detailed insights. Figure 22 confirms Hjorth complexity as the most important feature, with top channels C3, Cz, P8, C4, and Fz. The right panel shows channel \times feature heatmap revealing interactions between electrode locations and feature types in model predictions.

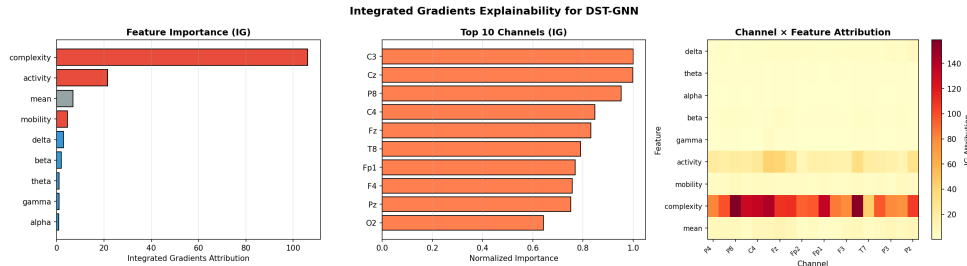


Figure 22: Integrated Gradients (IG): feature importance (left), top channels (center), channel \times feature (right)

Figure 23 shows the edge importance matrix displayed in two panels. The left panel shows the 19×19 importance matrix with cream-red color scale (0.0-1.0), where darker colors indicate higher importance. The right panel displays a bar chart of 15 most important connections (all approaching importance 1.0): Fz-Fp2, P8-Fz, C4-Fz, Cz-Fz, Fz-Fp1, Fz-F7, C4-T7, Fz-T7, C4-Pz, C4-O1, P8-F4, Cz-Fp2, Fz-C3, C4-P3, and P8-Cz. Dominance of connections involving Fz confirms the central role of frontal-midline cortex in classification. This Integrated Gradients-based analysis approach aligns with explainability methodology developed by Sujatha Ravindran and Contreras-Vidal (2023) for EEG model interpretation.

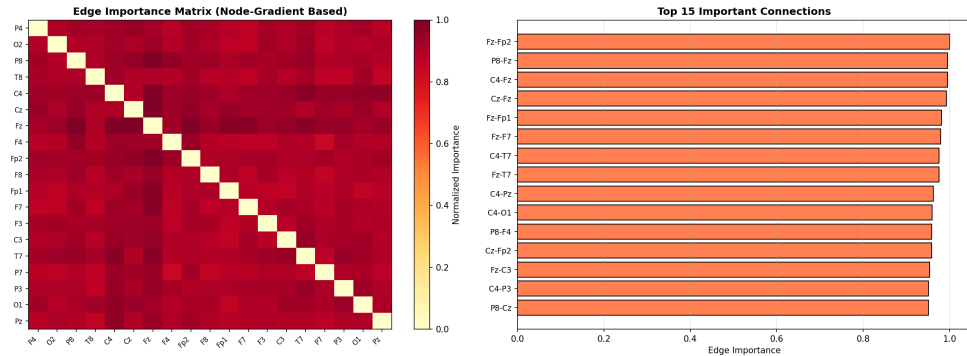


Figure 23: Edge importance matrix (left) and top 15 important connections (right)

Figure 24 presents PLI and wPLI comparison showing average correlation of 0.623, with wPLI producing $2.5\times$ higher connectivity values. wPLI is more robust to noise at 0° and 180° phase differences, making it a better choice for EEG connectivity analysis with high volume conduction potential.

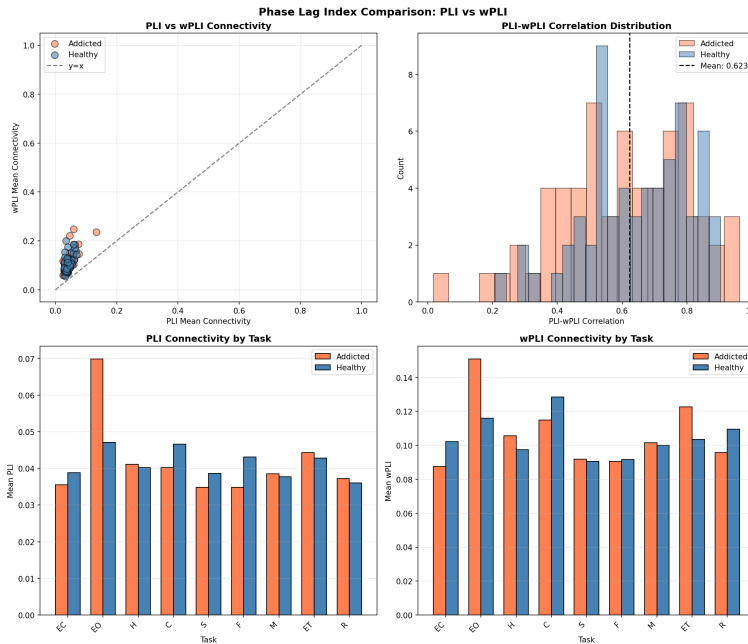


Figure 24: PLI vs wPLI comparison: scatter plot, correlation distribution, and connectivity per task

The results of this research have significant implications. First, DST-GNN provides an objective neuroscience-based screening tool that can complement self-report methods. High recall (85.71%) ensures minimization of false negatives. Second, identification of trait-level biomarkers (Cz-T7 connectivity) opens the possibility of detection without pornographic stimulus exposure. Third, identification of frontal-central regions can inform development of more targeted neurofeedback interventions. However, this research still has several limitations. First, small sample size ($N=14$) limits generalizability and causes high variability. Second, the dataset comes from a single center so cross-cultural validation is needed. Third, age range is limited (13-15 years). Fourth, the model has not been validated on real-time data.

4 Conclusion

This study successfully developed a Dynamic Spatio-Temporal Graph Neural Network (DST-GNN) for detecting pornography addiction in adolescents based on EEG signals. DST-GNN achieves F1-Score of $71.00\% \pm 12.10\%$ with recall 85.71%, a 104% improvement compared to the best baseline. Ablation study confirms temporal contribution (21%) and PLI graph construction (57%). Frontal-central regions (Fz, Cz, C3, C4) are identified as most discriminative with Beta contribution 58.9% and Hjorth 31.2%. Cz-T7 connectivity shows consistent patterns as a trait-level biomarker. These results contribute to child protection efforts by providing an objective screening tool. Future research is suggested to validate on larger datasets with Indonesian population, develop real-time systems, and integrate with neurofeedback protocols.

Acknowledgments

The authors would like to express their gratitude to Dr. Kang and the team at Taylor’s University for making the public dataset available via Mendeley Data. We also extend our appreciation to Yayasan Kita dan Buah Hati (YKBH) Jakarta for their contributions to the data collection process. This research was conducted in support of the mandate of Law No. 35 of 2014 regarding Child Protection.

Author Contributions

Achmad Ardani Prasha: Conceptualization, Methodology, Software, Validation, Formal analysis, Investigation, Data curation, Writing - original draft, Visualization. **Clavino Ourizqi Rachmadi:** Methodology, Validation, Formal analysis, Writing - review & editing. **Sabrina Laila Mutiara:** Methodology, Validation, Writing - review & editing. **Hilman Syachr Ramadhan:** Validation, Writing - review & editing. **Chareyl Reinalyta Borneo:** Validation, Writing - review & editing. **Saruni Dwiasnati:** Supervision, Project administration, Writing - review & editing.

References

- Abadal, S., Galván, P., Mármol, A., Mammone, N., Ieracitano, C., Lo Giudice, M., Salvini, A., and Morabito, F. C. Graph neural networks for electroencephalogram analysis: Alzheimer's disease and epilepsies use cases. *Neural Networks*, 181:106792, 2025.
- Adarsh, H. and Sahoo, S. Pornography and its impact on adolescent/teenage sexuality. *Journal of Psychosexual Health*, 5(1):35–39, 2023.
- Algarni, M., Saeed, F., Al-Hadhrani, T., Ghabban, F., and Al-Sarem, M. Deep learning-based approach for emotion recognition using electroencephalography (EEG) signals using bi-directional long short-term memory (Bi-LSTM). *Sensors*, 22(8):2976, 2022.
- Allgaier, J. and Pryss, R. Cross-validation visualized: A narrative guide to advanced methods. *Machine Learning and Knowledge Extraction*, 6(2):1378–1388, 2024.
- Almohammadi, A. and Wang, Y. K. Revealing brain connectivity: Graph embeddings for EEG representation learning and comparative analysis of structural and functional connectivity. *Frontiers in Neuroscience*, 17:1288433, 2024.
- Bouhadja, A. and Bouramoul, A. A review on recent machine learning applications for addiction disorders. In *4th International Conference on Pattern Analysis and Intelligent Systems (PAIS)*, pages 1–8, 2022.
- Brand, M., Young, K. S., Laier, C., Wölfling, K., and Potenza, M. N. Integrating psychological and neurobiological considerations regarding the development and maintenance of specific Internet-use disorders: An Interaction of Person-Affect-Cognition-Execution (I-PACE) model. *Neuroscience and Biobehavioral Reviews*, 71:252–266, 2016.
- Brand, M., Wegmann, E., Stark, R., Müller, A., Wölfling, K., Robbins, T. W., and Potenza, M. N. The Interaction of Person-Affect-Cognition-Execution (I-PACE) model for addictive behaviors: Update, generalization to addictive behaviors beyond internet-use disorders, and specification of the process character of addictive behaviors. *Neuroscience & Biobehavioral Reviews*, 104:1–10, 2019.
- Chaddad, A., Wu, Y., Kateb, R., and Bouridane, A. Electroencephalography signal processing: A comprehensive review and analysis of methods and techniques. *Sensors*, 23(14):6434, 2023.
- Cho, K., Van Merriënboer, B., Gulcehre, C., Bahdanau, D., Bougares, F., Schwenk, H., and Bengio, Y. Learning phrase representations using RNN encoder-decoder for statistical machine translation. In *Conference on Empirical Methods in Natural Language Processing (EMNLP)*, pages 1724–1734, 2014.
- Cui, J., Yuan, L., Wang, Z., Li, R., and Jiang, T. Towards best practice of interpreting deep learning models for EEG-based brain computer interfaces. *Frontiers in Computational Neuroscience*, 17:1232925, 2023.
- Faisal, N. A., Johari, K. S. K., Amat, M. I., and Yusof, R. Pornography addiction on adolescent: A systemic review of reported impact on brain and sexual behavior. *International Journal of Academic Research in Business and Social Sciences*, 12(6):2028–2041, 2022.
- Farahani, F. V., Fiok, K., Lahijanian, B., Karwowski, W., and Douglas, P. K. Explainable AI: A review of applications to neuroimaging data. *Frontiers in Neuroscience*, 16:906290, 2022.
- Graña, M. and Morais-Quilez, I. A review of graph neural networks for electroencephalography data analysis. *Neurocomputing*, 562:126901, 2023.
- Hjorth, B. EEG analysis based on time domain properties. *Electroencephalography and Clinical Neurophysiology*, 29(3):306–310, 1970.
- Huang, H. W., Li, P. Y., Chen, M. C., Chang, Y. X., Liu, C. L., Chen, P. W., Lin, Q., Lin, C., Huang, C. M., and Wu, S. C. Classification of internet addiction using machine learning on electroencephalography synchronization and functional connectivity. *Psychological Medicine*, 55:e148, 2025.

- Jusseume, K. and Valova, I. Brain age prediction/classification through recurrent deep learning with electroencephalogram recordings of seizure subjects. *Sensors*, 22(21):8112, 2022.
- Kang, X., Handayani, D. O. D., Abdul Rahman, A. W., and Agastya, I. M. A. Electroencephalogram (EEG) dataset with pornographic content exposure in adolescents. *Mendeley Data*, V5, 2021.
- Kementerian PPPA. *Survei Nasional Pengalaman Hidup Anak dan Remaja (SNPHAR)*. Kementerian Pemberdayaan Perempuan dan Perlindungan Anak, Jakarta, 2021.
- Klepl, D., Wu, M., and He, F. Graph neural networks in EEG-based emotion recognition: A survey. *IEEE Transactions on Neural Systems and Rehabilitation Engineering*, 32:493–503, 2024.
- Krukow, P., Rodríguez-González, V., Kopiś-Posiej, N., Gómez, C., and Poza, J. Tracking EEG network dynamics through transitions between eyes-closed, eyes-open, and task states. *Scientific Reports*, 14(1):17442, 2024.
- Liu, Z. and Zhao, J. Leveraging deep learning for robust EEG analysis in mental health monitoring. *Frontiers in Neuroinformatics*, 18:1494970, 2025.
- Polat, H. Brain functional connectivity based on phase lag index of electroencephalography for automated diagnosis of schizophrenia using residual neural networks. *Journal of Applied Clinical Medical Physics*, 24(7):e14039, 2023.
- Prantner, S., Espino-Payá, A., Pastor, M. C., Giménez-García, C., Kroker, T., Ballester-Arnal, R., and Junghöfer, M. Magnetoencephalographic correlates of pornography consumption: Associations with indicators of compulsive sexual behaviors. *International Journal of Clinical and Health Psychology*, 24(4):100524, 2024.
- Privara, M. and Bob, P. Pornography consumption and cognitive-affective distress. *The Journal of Nervous and Mental Disease*, 211(8):641–646, 2023.
- Raveendran, S., S, K., A G, R., Kenchaiah, R., Sahoo, J., Kumar, S., M K, F., Mundlamuri, R. C., Bansal, S., V S, B., and R, S. Functional connectivity in EEG: A multiclass classification approach for disorders of consciousness. *Frontiers in Neuroscience*, 19:1550581, 2025.
- Shu, Q., Tang, S., Wu, Z., Feng, J., Lv, W., Huang, M., and Xu, F. The impact of internet pornography addiction on brain function: A functional near-infrared spectroscopy study. *Frontiers in Human Neuroscience*, 19:1477914, 2025.
- Stam, C. J., Nolte, G., and Daffertshofer, A. Phase lag index: Assessment of functional connectivity from multi channel EEG and MEG with diminished bias from common sources. *Human Brain Mapping*, 28(11):1178–1193, 2007.
- Sujatha Ravindran, A. and Contreras-Vidal, J. An empirical comparison of deep learning explainability approaches for EEG using simulated ground truth. *Scientific Reports*, 13(1):17709, 2023.
- Sun, S., Yang, J., Chen, Y. H., Miao, J., and Sawan, M. EEG signals based internet addiction diagnosis using convolutional neural networks. *Applied Sciences*, 12(13):6297, 2022.
- Veličković, P., Cucurull, G., Casanova, A., Romero, A., Liò, P., and Bengio, Y. Graph attention networks. In *International Conference on Learning Representations (ICLR)*, 2018.
- Venu, K. and Natesan, P. Hybrid optimization assisted channel selection of EEG for deep learning model-based classification of motor imagery task. *Biomedical Engineering / Biomedizinische Technik*, 69(2):125–140, 2024.
- Walther, D., Viehweg, J., Hauelsen, J., and Mäder, P. A systematic comparison of deep learning methods for EEG time series analysis. *Frontiers in Neuroinformatics*, 17:1067095, 2023.
- Welch, P. The use of fast Fourier transform for the estimation of power spectra: A method based on time averaging over short, modified periodograms. *IEEE Transactions on Audio and Electroacoustics*, 15(2):70–73, 1967.

- Xue, Q., Song, Y., Wu, H., Cheng, Y., and Pan, H. Graph neural network based on brain inspired forward-forward mechanism for motor imagery classification in brain-computer interfaces. *Frontiers in Neuroscience*, 18:1309594, 2024.
- Yan, Y., Zhao, A., Ying, W., Qiu, Y., Ding, Y., Wang, Y., Xu, W., and Deng, Y. Functional connectivity alterations based on the weighted phase lag index: An exploratory electroencephalography study on Alzheimer's disease. *Current Alzheimer Research*, 18(6):513–522, 2021.